Flow Unsteadiness Considerations in High-Alpha Testing

L. E. Ericsson*
Lockheed Missiles & Space Company, Inc., Sunnyvale, California

An analysis has been performed of the experimentally observed asymmetric flow separation on slender forebodies, a flow phenomenon encountered by high-performance aircraft and missiles performing advanced maneuvers. It is found that, even at the low angular rates associated with a coordinated turn, for example, the usual methods of modifying static test results to account for the influence of modest angular rates cannot be applied. The reason is the existence of two types of flow unsteadiness—one independent of and the other highly dependent on the vehicle motion. In a static high-alpha test, the motion-independent unsteadiness of the slender forebody vortices will generate time-averaged (static) asymmetric loads that are of lesser magnitude than the "frozen" instantaneous asymmetric loads. In a high-alpha flight maneuver, on the other hand, the motion-dependent unsteadiness can cause the vortex-induced side force to attain and stay at its maximum value for an extended period of time. As a consequence, only test data obtained with a rotary-rig type of apparatus that can generate coning or rolling motions will provide the vehicle designer with the correct asymmetric loads.

Nomenclature

c = cross-sectional chord length, = d for a circular cylinder
d = cylinder diameter
h = cross-sectional height or thickness
ℓ = cross-sectional lift; coefficient $c_\ell = \ell/(\rho_\infty U_\infty^2/2)c$
M = Mach number
P = static pressure; coefficient $C_p = (P - P_\infty)/(p_\infty U_\infty^2/2)$
p = rotation or spin rate
Re = Reynolds number, $= U_\infty c/\nu_\infty$
S = reference area, $= \pi d^2/4$
t = time
U = freestream velocity
U_W = wall velocity
x = axial distance from apex
Y = side force; coefficient $C_Y = Y/(\rho_\infty U_\infty^2/2)S$; $c_y = dC_Y/d\xi$
Y^* = sideforce of forebody, forward of rotation axis; coefficient $C_Y^* Y^*/(\rho_\infty U_\infty^2/2)S$
α = angle of attack
β = local side slip angle, $\approx U_w/U_\infty$
Δ = lateral differential
ν = kinematic viscosity
ξ = dimensionless coordinate, $\xi = x/c$
ρ = fluid density
ϕ = roll angle
φ = peripheral angle, = 0 at the stagnation point
ψ = coning angle

Subscripts

max = maximum
W = wall
∞ = freestream conditions

Derivative Symbols

$\dot{\psi} = \partial\psi/\partial t$, $\ddot{\psi} = \partial^2\psi/\partial t^2$

Presented as Paper 88-0057 at the AIAA 26th Aerospace Sciences Meeting, Reno, NV, Jan. 12-15, 1988; received Feb. 12, 1988; revision received June 20, 1988.

*Senior Consulting Engineer. Fellow AIAA.

Introduction

THE intermittent, unsteady character of asymmetric forebody vortices has already been observed by Allen and Perkins,[1] who found that the asymmetry changed between its two extremes in an aperiodic manner. Further investigations by Gowen[2] showed that the lateral pressure difference $\Delta C_p = C_p(t) - C_{p\text{mean}}$ *at* $\varphi = \pm 157$ deg on the leeside varied in a random, aperiodic manner (Fig. 1). More recent test results[3,4] show similar intermittent, asymmetric vortex characteristics. Figure 1 illustrates the relation between the static, time-averaged value of the side force and the instantaneous one.

Besides presenting a possible forcing function of the buffet type, the unsteadiness of the asymmetric vortices also indicates a certain tendency for the coupling with the vehicle motion described in Refs. 5 and 6. A similar concern was expressed by Gowen and Perkins[7]: "It is realized that for full-scale vehicles in flight there exists the possibility of coupling between the shedding of the wake vorticies and the movement of the aircraft." How the angle of attack affects the vortex unsteadiness is discussed at length in Ref. 8.

Moving Wall Effects

The coupling between vehicle motion and forebody vortex shedding occurs through the so-called moving wall effect. The classic Magnus lift on a rotating circular cylinder represents a well-established case of moving wall effects. The experimental results presented by Swanson[9] will be used as a reference when discussing other types of moving wall effects. The wall-jet-like effect of the moving wall is illustrated in Fig. 2 for laminar (initial) flow conditions. On the top, the downstream moving wall effects fill out the boundary-layer velocity profile, thereby delaying flow separation; on the bottom, the upstream moving wall effects promote separation. As long as the flow remains laminar, the net result is a positive Magnus lift (for $U_w/U_\infty < 0.3$ in Fig. 2). However, when the wall velocity exceeds a critical ratio (e.g., $U_w/U_\infty = 0.3$ for $Re = 0.128 \times 10^6$ in Fig. 2), the adverse, upstream moving wall effect on the bottom half causes transition to occur before separation, changing it from the subcritical toward the supercritical type and resulting in a net lift force that is negative. This so-called Magnus lift reversal will occur at lower and lower U_w/U_∞ as Re is increased, until the initial moving wall effect is to generate negative lift when $U_w/U_\infty > 0$.

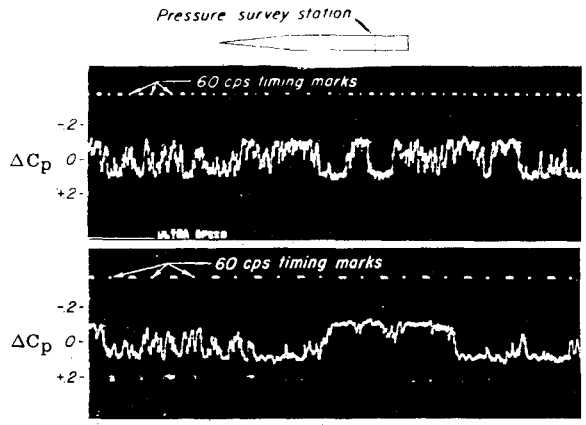

Fig. 1 Two time traces of the differential pressure at $\varphi = \pm 157$ deg and $\xi = 10.6$ on a cone-cylinder body ($\alpha = 23.7$ deg, $M_\infty = 1.45$, and $Re = 0.5 \times 10^6$ (from Ref. 2).

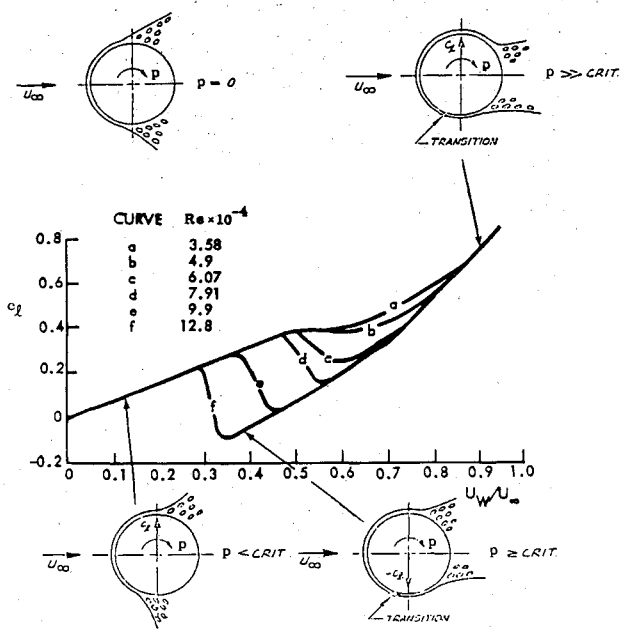

Fig. 2 Magnus lift characteristics of a circular cylinder for initially subcritical flow conditions.

Slender Bodies at High Angles of Attack

Similar moving wall effects occur on bodies of revolution at high angles of attack. Even a modest spin rate has a large effect on the side force of a cone-cylinder body[10] (Fig. 3). The experimental results[11] in Fig. 4 show how powerful the three-dimensional moving wall effects can be. The authors describe how only a slight push was needed to establish the coning motion in one direction or the other, regardless of the fact that the measured static yawing moment was biased in one direction due to nose micro-asymmetries.[12] That is, the motion dominated over the static asymmetry, locking in the vortex asymmetry in the direction of the body motion, driving it.

In the case of the coning motion, the moving wall effects act as follows on the translating cross section (Fig. 5): the lateral motion causes the flow separation to be delayed on the advancing side and promoted on the retreating side, the important moving wall effects being those generated near the flow stagnation point. Thus, the motion produces a force that drives it until an equilibrium coning rate is reached, where the driving moment generated by the asymmetric separation is balanced by the drag-generated damping moment.

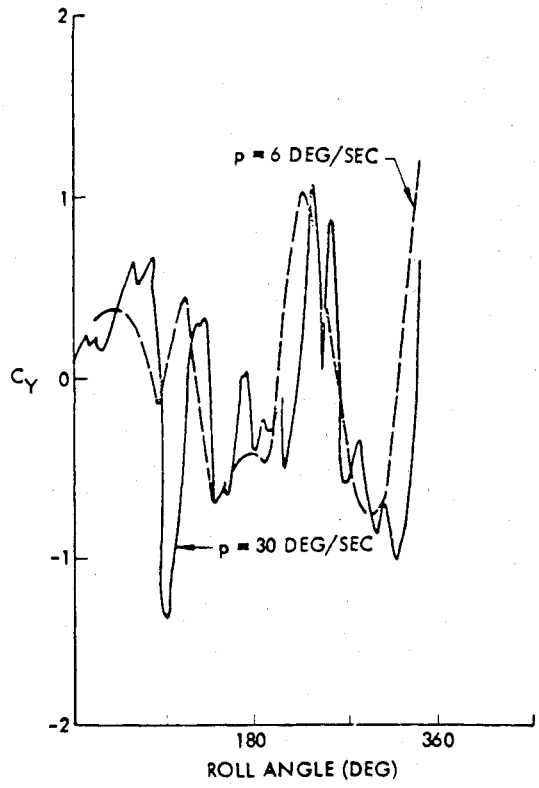

Fig. 3 Effect of spin rate and roll angle on the side force of a cone-cylinder.[10]

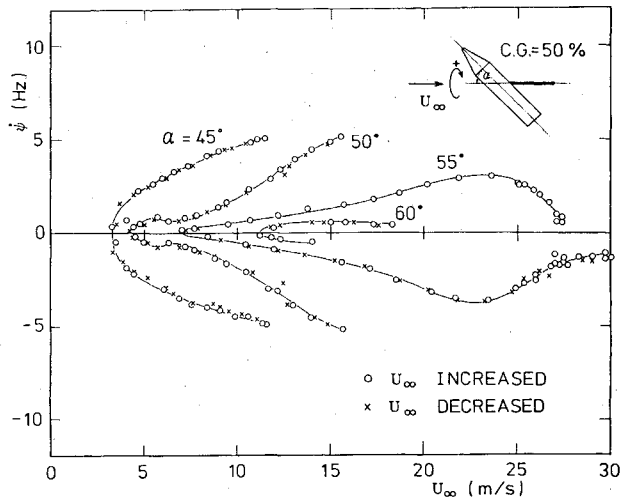

Fig. 4 Dual coning characteristics of a cone-cylinder.[11]

Similar moving wall effects on transition can explain the oscillatory coning behavior observed experimentally for a cone-cylinder body flying backward[11] (Fig. 6). The mirror symmetry of the limiting coning rates is very similar to that obtained for the regular nose-forward orientation (Fig. 4). However, in this case no exterior push was needed to change the coning direction. The measured acceleration and coning rates are shown in Fig. 7. It can be seen that, when a certain limiting coning rate is reached, the acceleration suddenly switches sign.

The fluid mechanical process can be described as follows, with the aid of the inserted flow sketches. Initially, flow asymmetry or minute surface irregularities set the separation asymmetry, initiating the coning motion. The coning-induced moving wall effects delay the laminar separation on the

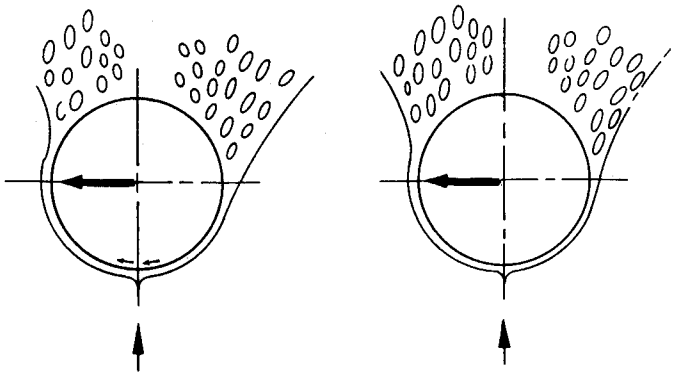

Fig. 5 Moving wall effects on a translating circular cross section.

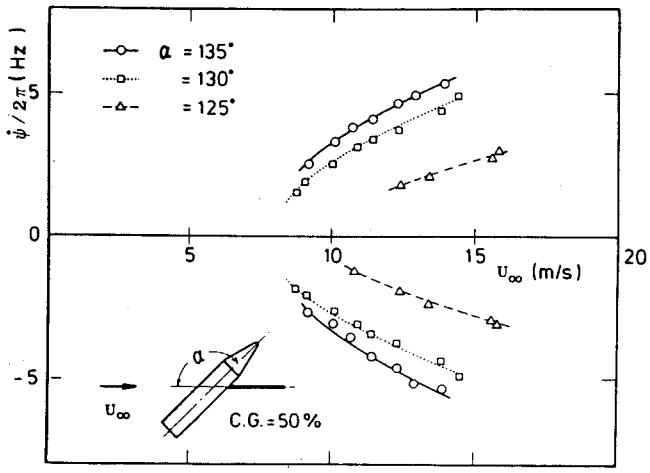

Fig. 6 Oscillatory coning of a circular cylinder.[11]

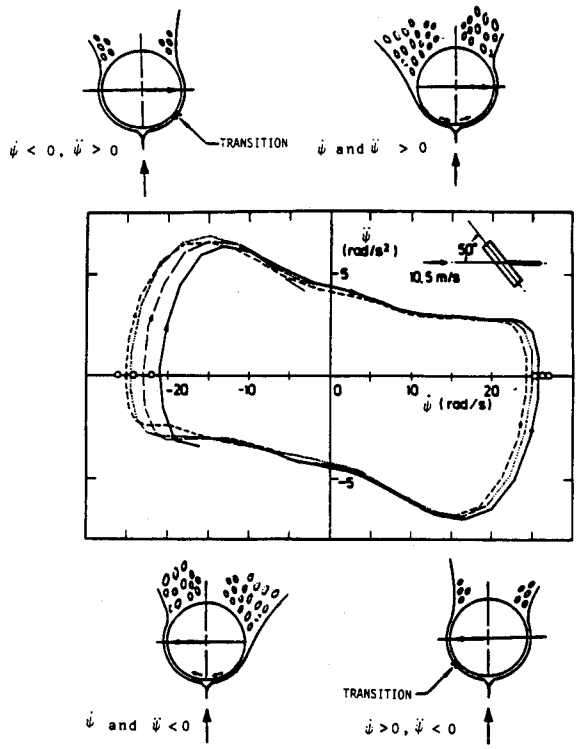

Fig. 7 Reversal of cylinder coning.

advancing side, resulting in positive coning velocity and spin acceleration ($\dot{\psi}$ and $\ddot{\psi} > 0$). However, the adverse upstream moving wall effect eventually causes boundary-layer transition on the retreating side, the effect being very similar to the one observed for the rotating cylinder[9] (Fig. 2). This reverses the vortex asymmetry and the coning motion starts to decelerate ($\dot{\psi} > 0, \ddot{\psi} < 0$). The coning reversal moves transition back into the wake on the new advancing side and the asymmetric laminar separation is re-established.

Eventually, transition occurs on the retreating side to cause critical/subcritical separation asymmetry, reversing the vortex asymmetry and decelerating the coning motion ($\dot{\psi} < 0, \ddot{\psi} > 0$). The process continually repeats itself, resulting in a self-reversing coning motion. A similar self-reversing spinning motion causes the observed wing rock generated by forebody vortices.[13,14]

Simulation Problems

In view of the strong interplay between Reynolds number and moving wall effects just demonstrated, Champigny's experimental results[15] (Fig. 8) give cause for the concerns expressed in Refs. 5 and 6 that in full-scale flight a vehicle maneuver could lock-in the flow separation asymmetry along the full length of a missile or aircraft forebody.

Getting back to the problem of wind-tunnel tests at high alpha, the experimental results[4] in Fig. 9 show how a reduction of the freestream turbulence from the 0.7% level of the Bristol tunnel (Fig. 9a) to the 0.01% of the RAE tunnel (Fig. 9b) eliminated the intermittent "flipping" of the vortex asymmetry. However, eliminating this high turbulence level did not change the effect of roll angle (Fig. 10), contrary to the authors' expectation.[4] They concluded that this affect is caused by micro-asymmetries[12] and persists even in presence of high turbulence levels.

The similar effects of Reynolds number and freestream turbulence implies, according to the above discussion, that even more dramatic changes of the asymmetric loads than those shown in Fig. 8 can be caused by nose micro-asymmetrics, as is also demonstrated by the measured effect of roll angle[16] (Fig. 11). The fact that the moving wall effect is more powerful than the forebody micro-asymmetry, as was illustrated in Figs. 4–7, can be understood when one realizes that the moving wall effect in these cases is the equivalent to having different effective Reynolds number flows on the port and starboard sides of the

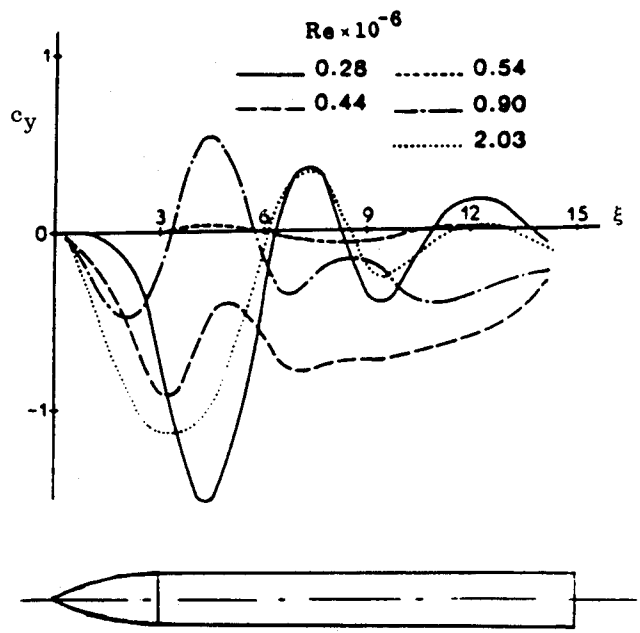

Fig. 8 Side force distribution at $\alpha = 50$ deg on an ogive-cylinder through the critical Reynolds number range.[15]

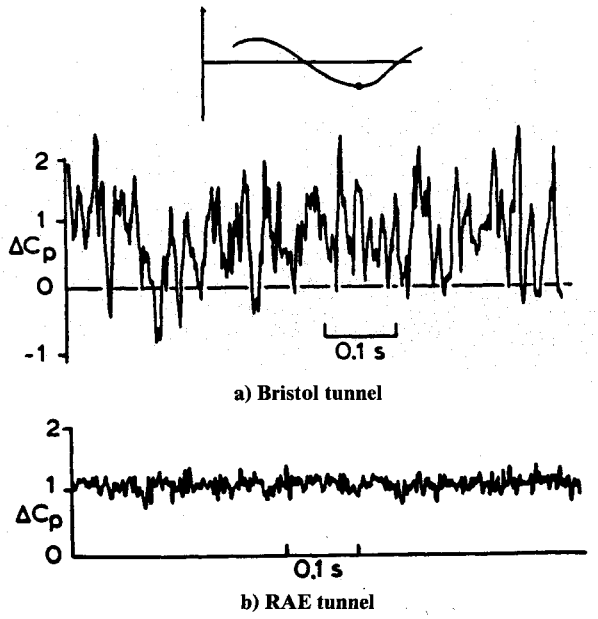

Fig. 9 Lateral leeside pressure differential at $\xi = 5$ on an ogive-cylinder at $\alpha = 60$ deg and $Re = 0.11 \times 10^6$ (from Ref. 4).

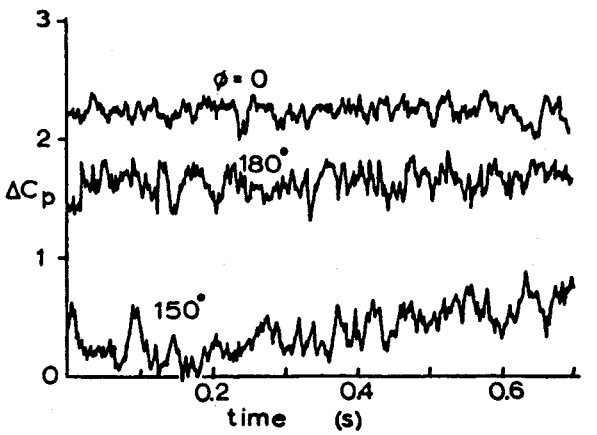

Fig. 10 Effect of roll angle on lateral pressure differential at $\xi = 4$ on an ogive-cylinder at $\alpha = 50$ deg and $Re = 0.10 \times 10^6$ (from Ref. 4).

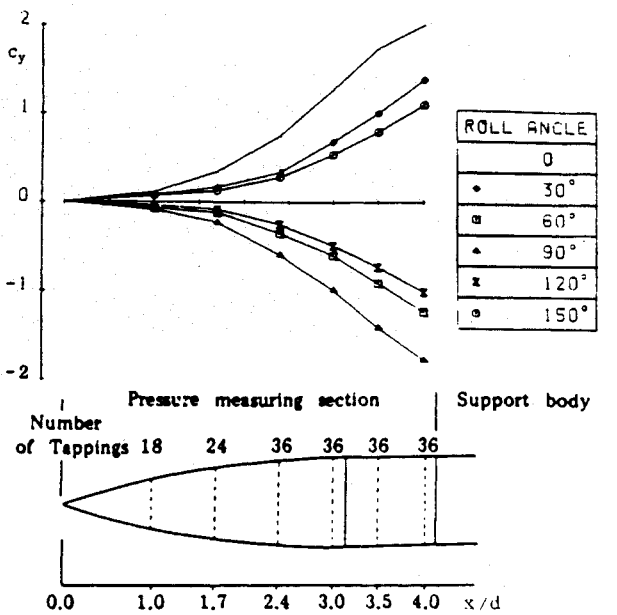

Fig. 11 Effect of roll angle on side force distribution at $\alpha = 50$ deg on an ogive-cylinder at $Re = 0.13 \times 10^6$ (from Ref. 16).

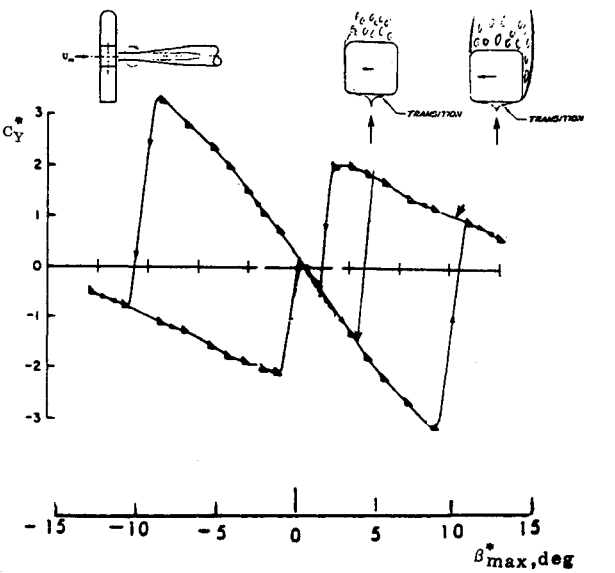

Fig. 12 Forebody side force characteristics of a square cross-section body in flat spin.[17]

body. Combining this with the effect of the uniform (flow) Reynolds number shown in Fig. 8, one can understand why the moving effect is so dominant. Equally large moving wall effects have also been measured on noncircular cross-sectional forebodies[17,18] (Fig. 12).

The conclusion to be drawn from the discussed experimental results is that great care has to be exercised when attempting to use static high-alpha test results for analysis of full-scale flight characteristics. In addition to the unsteady flow effects of turbulence type, illustrated in Fig. 9, one has to consider the fact that the support-model structure is likely to exhibit laterial bending oscillations.[19] As they are harmonic in nature, they will produce a zero time average of the asymmetric load. That is, the situation can be even worse than what is illustrated in Figs. 1 and 9a.

Thus, only forced coning tests, performed with a rotary rig, can supply the correct asymmetric loads at high angles of attack, provided that proper consideration is given to the usual scaling[20-23] and support interference[24,25] problems. In addition to this stationary coning data, one needs experimental results for small perturbations in pitch, yaw, and roll relative to the coning motion for a complete description of the high-alpha aerodynamics of an advanced aircraft.[26] Test rigs that can supply this complete information are presently not available. However, a special coning rig with a tilted axis exists, which produces an oscillatory coning motion.[27] It provides a restricted but still useful form of perturbation from the steady coning motion.

Conclusions

Analysis of available experimental results has led to the following conclusions in regard to the use of "static" test data to describe the aerodynamics of high-performance aircraft and missiles maneuvering at high angles of attack:

1) Flow separation is not a static flow phenomenon. Associated with flow separation is flow unsteadiness of two basic types: one is motion independent, generating the aerodynamic forcing function usually connected with the buffet type of vehicle response, and the other highly motion dependent, often generating negative aerodynamic damping.

2) In a static high-alpha test the motion-independent unsteadiness of vortices generated by slender forebodies will cause

the measured time-averaged (static) side force and associated yawing moment to be of lesser magnitude than the instantaneous (maximum) side force and associated moment. On the other hand, in a high-alpha flight maneuver, the motion-dependent unsteadiness can cause the vortex-induced side force and moment to stay at the maximum levels for an extended period of time.

3) In order to obtain "static" or quasi-steady vortex-induced aerodynamic characteristics that can be applied to a maneuvering full-scale vehicle, one needs to use test rigs that provide coning and/or rolling motions of the model.

References

[1]Allen, H. J. and Perkins, E. W., "Characteristics of Flow Over Inclined Bodies of Revolution," NACA RMA50L07, March 1951.

[2]Gowen, F. E., "Buffeting of a Vertical Tail on an Inclined Body at Supersonic Mach Number," NACA RMA53A09, March 1953.

[3]Lamont, P. J. and Hunt, B. L., "Pressure and Force Distributions on a Sharp-Nosed Circular Cylinder at Large Angles of Inclination to a Uniform Stream," *Journal of Fluid Mechanics,* Vol. 76, Pt. 3, 1976, pp. 519–559.

[4]Hunt, B.L. and Dexter, P. C., "Pressures on a Slender Body at High Angle of Attack in a Very Low Turbulence Level Air Stream," AGARD CP-2457, Paper 17, Jan. 1979.

[5]Ericsson, L. E. and Reding, J. P., "Steady and Unsteady Vortex-Induced Asymmetric Loads on Slender Vehicles," *Journal of Spacecraft and Rockets,* Vol. 18, March–April 1981, pp. 97–109.

[6]Ericsson, L. E. and Reding, J. P., "Dynamics of Forebody Flow Separation and Associated Vortices," *Journal of Aircraft,* Vol. 22, April 1985, pp. 329–335.

[7]Gowen, F. E. and Perkins, E. W., "A Study of the Effects of Body Shape on the Vortex Wakes of Inclined Bodies at a Mach Number of 2," NACA RM A53I17, Dec. 1953.

[8]Ericsson, L. E., "Vortex Unsteadiness on Slender Bodies at High Incidence," *Journal of Spacecraft and Rockets,* Vol. 24, July–Aug. 1987, pp. 318–325.

[9]Swanson, W. M., "The Magnus Effect: A Summary of Investigations to Date," *Journal of Basic Engineering*, Vol. 83, Sept. 1961, pp. 461–470.

[10]Atraghji, E. G., "The Influence of Mach Number, Semi-Nose Angle and Roll Rate on the Development of the Forces and Moments Over a Series of Long Slender Bodies of Revolution at Incidence," National Research Council, Ottawa, Canada, NAE Data Rept. 5x5/0020, 1967.

[11]Yoshinaga, T., Tate, A., and Inoue, K., "Coning Motion of Slender Bodies at High Angles of Attack in Low Speed Flow," AIAA Paper 81-1899, Aug. 1981.

[12]Ericsson, L. E. and Reding, J. P., "Asymmetric Vortex Shedding from Bodies of Revolution," *AIAA Progress in Astronautics and Aeronautics: Tactical Missile Aerodynamics,* Vol. 104, edited by M. J. Hemsch and J. N. Nielsen, AIAA, Washington, DC, 1986, pp. 243–296.

[13]Brandon, J. M. and Nguyen, L. T., "Experimental Study of Effects of Forebody Geometry on High Angle of Attack Static and Dynamic Stability," AIAA Paper 86-0331, Jan. 1986.

[14]Ericsson, L. E., "Wing Rock Generated by Forebody Vortices," AIAA Paper 87-0268, Jan. 1987.

[15]Champigny, P., "Reynolds Number Effect on the Aerodynamic Characteristics of an Ogive-Cylinder at High Angles of Attack," AIAA Paper 84-2176, Aug. 1984.

[16]Dexter, P. C., "Final Report on an Analysis of the Data Obtained from Low Speed Wind Tunnel Tests of Three Calibre Tangent-Ogive Nose and Cylinder Combination at High Angles of Incidence," Bristol Aerospace, Dynamics Group, Rept. BT 15034, July 1983.

[17]Malcolm, G. N. and Clarkson, M. H., "Wind Tunnel Testing with a Rotary-Balance Apparatus to Simulate Aircraft Spin Motions," *Proceedings of the AIAA 9th Aerodynamic Testing Conference,* June 1976, pp. 143–146.

[18]Ericsson, L. E., "Aerodynamic Characteristics of Noncircular Bodies in Flat Spin and Coning Motions," *Journal of Aircraft,* Vol. 22, May 1985, pp. 387–392.

[19]Ericsson, L. E., "Lateral Oscillations of Sting-Mounted Models at High Alpha," AIAA Paper 89-0047, to be presented.

[20]Ericsson, L. E. and Reding, J. P., "Scaling Problems in Dynamic Tests of Aircraft-Like Configurations," AGARD CP-227, Paper 25, Feb. 1978.

[21]Ericsson, L. E. and Reding, J. P., "Reynolds Number Criticality in Dynamic Tests," AIAA Paper 78-166, Jan. 1978.

[22]Ericsson, L. E. and Reding, J. P., "Dynamic Simulation Through Analytic Extrapolation," *Journal of Spacecraft and Rockets,* Vol. 19, March–April 1982, pp. 160–166.

[23]Ericsson, L. E. and Reding, J. P., "Analytic Extrapolation to Full Scale Aircraft Dynamics," *Journal of Aircraft*, Vol. 21, March 1984, pp. 222–224.

[24]Ericsson, L. E. and Reding, J. P., "Review of Support Interference in Dynamic Tests," *AIAA Journal*, Vol. 21, Dec. 1983, pp. 1652–1666.

[25]Ericsson, L. E., "Dynamic Support Interference in High Alpha Testing," *Journal of Aircraft,* Vol. 23, Dec. 1986, pp. 889–896.

[26]Tobak, M. and Schiff, L. B., "Generalized Formulation of Nonlinear Pitch-Yaw-Roll Coupling: Part I – Nonaxisymmetric Bodies," *AIAA Journal,* Vol. 13, March 1975, pp. 323–326; "Part II – Nonlinear Coning-Rate Dependence," *AIAA Journal,* Vol. 13, March 1975, pp. 327–332.

[27]Tristant, D. and Renier, O., "Récents Développements des Techniques de Simulation Dynamique Appliquées a l'Identification des Parameters de Stabilité," AGARD CP-386, Paper 22, Nov. 1985.